MINAR International Journal of Applied Sciences and Technology
ISSN: 2717-8234
Article type: Research Article

Received: 09/10/2022 **Accepted:** 28/10/2022 **Published:** 01/12/2022

ESTIMATION OF POWER DEPOSITION IN ICP REACTOR

Dawser Hussain GHAYB[1]

University of Baghdad, Iraq

Abstract

In the present paper, the power deposited in the inductively coupled radiofrequency (RF) discharges is investigated by a two-dimensional fluid model. The discharge process was sustained in Ar / O2 gases mixture with 50:50 percentage of mixture volume. The discharge properties in the mixture obtained. An operating RF frequency of 13.56 MHz and applied voltage of 20 kV are simulated. A simple known international design of the reactor was chosen with 5 turn coil. Input power of the reactor was 1500 W. This numerical study done using plasma multiphysics model. Results show that the power deposition shows enhancement in behavior as the pressure increased.

Keywords: ICP Plasma, Ar Gas, O2 Gas, Power Deposition, Electric Potential.

http://dx.doi.org/10.47832/2717-8234.13.13

[1] dawserhg_phys@csw.uobaghdad.edu.iq, https://orcid.org/0000-0001-9989-1779

1. Introduction:

Plasma, the fourth state of matter, occupies a great importance in many fields. It has many applications in medicine, industry, food processing, and environment [1-4]. Many researches study plasma diagnostics and conditions improvements in different plasma generation devices [5-6]. Inductively coupled plasma ICP reactors are widely used for microelectronic device fabrication processes, i.e. etching and deposition [7]. ICP reactors known to be operated at low gas pressure (<50 mTorr). This is necessary to improve uniformity and high plasma density. Also it is important to deliver a high density of ions and radicals to the wafer surface in which are widely used for microelectronic devices fabrication [8]. In this reactor, plasma is produced in the first state using a static electric field between the segments of the coil in a capacitive manner. This is called as E-mode. Other mode which is called as H – mode in which the plasma is generated according to the electromagnetic fields presented from the same coil. The H- mode is an inductive mode becomes relevant at higher powers. The discharges generated by E-mode and the transition can have developed with increasing the applied power, that is clear shown when there is a sudden increase in discharge density [9-11]. The inductively coupled discharges (ICPs) use predominantly parallel electric field for power deposition into the plasma. As the radial electric field for the over dense plasmas, which is normally the case, decays into the plasma with the skin-effect, the power absorption can be more or less uniform (when the skin depth is large compared to the inter electrode gap) or strongly localized otherwise. [12]. Many dimensional models have been work out to made a simulation to the ICP reactors. In all these models azimuthally symmetric profiles for power deposition and chemical species densities were assumed [13-16].

Little studies were done to ICP plasma reactor while Power deposition was absent from view. Horia E et al use numerical simulation to estimate the minim power needed in the ICP reactor used [17]. Hyo Lee [18] made study to the hysteresis physics in plasmas of ICP plasmas. Vinogradov et al [19] studying the plasma density in the ICP plasma reactor by using probe diagnostics. Quan and Annemiie [20] study the effect of capacitive electrical asymmetry on the reactor plasma parameters such as ion energy and ion flux [20]. In the present paper, an investigation of the power deposited in inductively coupled plasma reactor were made by using numerical simulation. This study will make a new view to one of the important parameter effect on the efficiency of the reactor.

2. Method:

Generally, inductively coupled discharges operate in certain conditions such as low pressures and high density. A high degree of anisotropy would be provided due to bombardment of low pressure ions which produced by high density plasma sources. This make the most popular applied sources are high density plasma one. In the present work, the mathematical model used computes the electron density and mean electron energy by solving the drift diffusion equations. The drift diffusion equations will be solved as a pair for the electron density and mean electron energy. The standard used equation is [21]:

$$\frac{\partial}{\partial t}(n_e) + \nabla \cdot [-n_e(\mu_e \bullet \mathbf{E}) - \mathbf{D}_e \bullet \nabla n_e] = R_e$$

$$\frac{\partial}{\partial t}(n_\varepsilon) + \nabla \cdot [-n_\varepsilon(\mu_\varepsilon \bullet \mathbf{E}) - \mathbf{D}_\varepsilon \bullet \nabla n_\varepsilon] + \mathbf{E} \cdot \Gamma_e = R_\varepsilon$$

Where n_e is the electron number density, D_e is electron diffusivity, μ_e is electron mobility, R_e is the electron source and R_ε represents the energy loss with respect to inelastic collisions. When there is a strong DC magnetic field, then the electron mobility will be in a tensor form as below:

$$\boldsymbol{\mu}_e^{-1} = \begin{bmatrix} \frac{1}{\mu_{dc}} & -B_z & B_y \\ B_z & \frac{1}{\mu_{dc}} & -B_x \\ -B_y & B_x & \frac{1}{\mu_{dc}} \end{bmatrix}$$

Since the actual mathematical form for the electron mobility cannot be written in a compact form so the inverse of. In the absence of the magnetic field, μ_{dc} represents the electron mobility. Computing electron diffusivity, energy diffusivity and mobility from the electron mobility by using the equation [21]:

$$\mathbf{D}_e = \mu_e T_e, \mu_\varepsilon = \left(\frac{5}{3}\right)\mu_e, \mathbf{D}_\varepsilon = \mu_\varepsilon T_e$$

To compute the coefficients R_e and R_ε in the above equations, it is necessary to use the plasma chemistry and especially rate coefficients. Poisson's Equation is used to estimates electrostatic field:

$$-\nabla \cdot \varepsilon_0 \varepsilon_r \nabla V = \rho$$

Where ρ represents the space charge density. ρ is computed automatically by the plasma chemistry derived in the model using the equation [21]:

$$\rho = q\left(\sum_{k=1}^{N} Z_k n_k - n_e\right)$$

For a non-magnetized plasma, non-polarized plasma, the produced induction currents are estimated within the frequency domain by applying the equation [22]:

$$(j\omega\sigma - \omega^2\varepsilon_0)\mathbf{A} + \nabla \times (\mu_0^{-1}\nabla \times \mathbf{A}) = \mathbf{J}^e$$

The plasma conductivity is estimated from the cold plasma approximation:

$$\sigma = \frac{n_e q^2}{m_e(\nu_e + j\omega)}$$

Where ν_e and ω are represent collisions frequency and the angular frequency respectively.

The discharge gas used in this work is a mixture of Ar and O2 gases with 50% percent. Argon is one of the simplest to be used at low pressures mechanisms due to complexity of the physics existing in an inductively coupled plasma. The oxygen gas used in the study due to is high actively ion species.

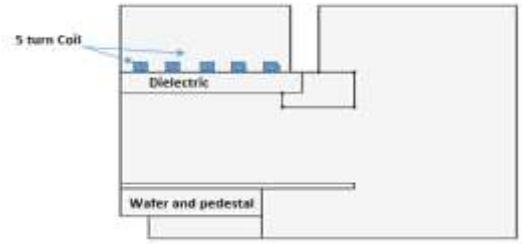

Figure 1. a 2D simple diagram of ICP reactor used in the simulation.

The two-dimensional axisymmetric schematic diagram of a commercial ICP etcher is given in Fig. 1. It shows that the reactor consists of 5 turn copper flat spiral coil supplied by a 13.56 MHz radio frequency (RF) power above the dielectric window generates plasma at low pressure. The dielectric used is quartz with dielectric constant equal to 4.6. The simulation boundary conditions of this system are 1.5 Pa and 1500 W in RF power, respectively.

Gas temperature set to be 300 K. since it is the more plasma used discharge gas, the plasma chemistry includes gas ionization reactions, excitation, recombination and attachment reactions. The species taken into account are electrons, molecules (Ar, O_2), ions (Ar+ , O_2+ , O_2 + , Ar O_2+), and neutrals (Ar* , O_2, O(2p), O(2s), O-). The reactions of electron impact collision and those of ions and neutral species are listed in Table 1.

The mesh build in an extra fine triangular mesh with number of elements equal to 25009, and it is distributed to layers and regions as a dense extremely fine in the coil region. Figure 2 shows the built mesh in the domain of study.

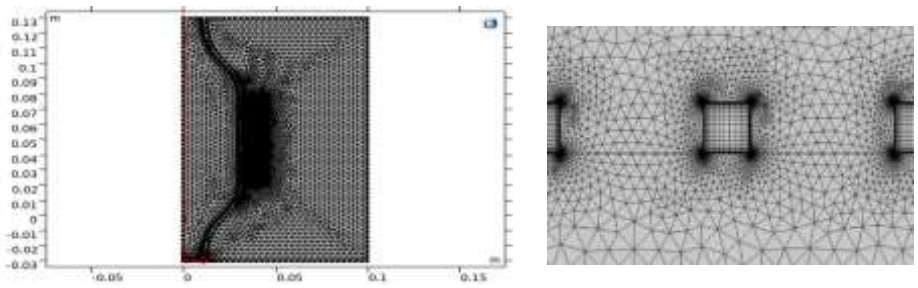

a. **b.**

Figure 2. The built mesh in the domain. a. the whole domain mesh. B. coil mesh.

The Coil set to the power while the walls grounded. The initial number density of electrons is to be 1×10^{15} cm^{-3}. With reduced electron mobility user defined. All the given equations are solved by using the ICP module of the COMSOL Multiphysics simulation package. The equations are discretized by the finite element logarithm formula method using linear element shape functions.

Results and Discussion:

In the present paper, a plasma diagnostic by studying the time evolution to electron number density, electron temperature and electric potential presented. Also, an estimation to the power loss and deposited in the inductively coupled plasma reactor also present.

Figure 3 shows the time evolution of electron number density along the reactor inner system. From figure, at time 1×10^{-8} s the electron number density was 3.5×10^{15} /m^3. As the time increased, the electron number density increased until reached 1.2×10^{20}/m^3 when the time was 0.01 s. this is a fact because the electron avalanche increased with time and made more collisions with molecules which results is more secondary electrons. The production of secondary electrons sustains the discharge and increase the electron density.

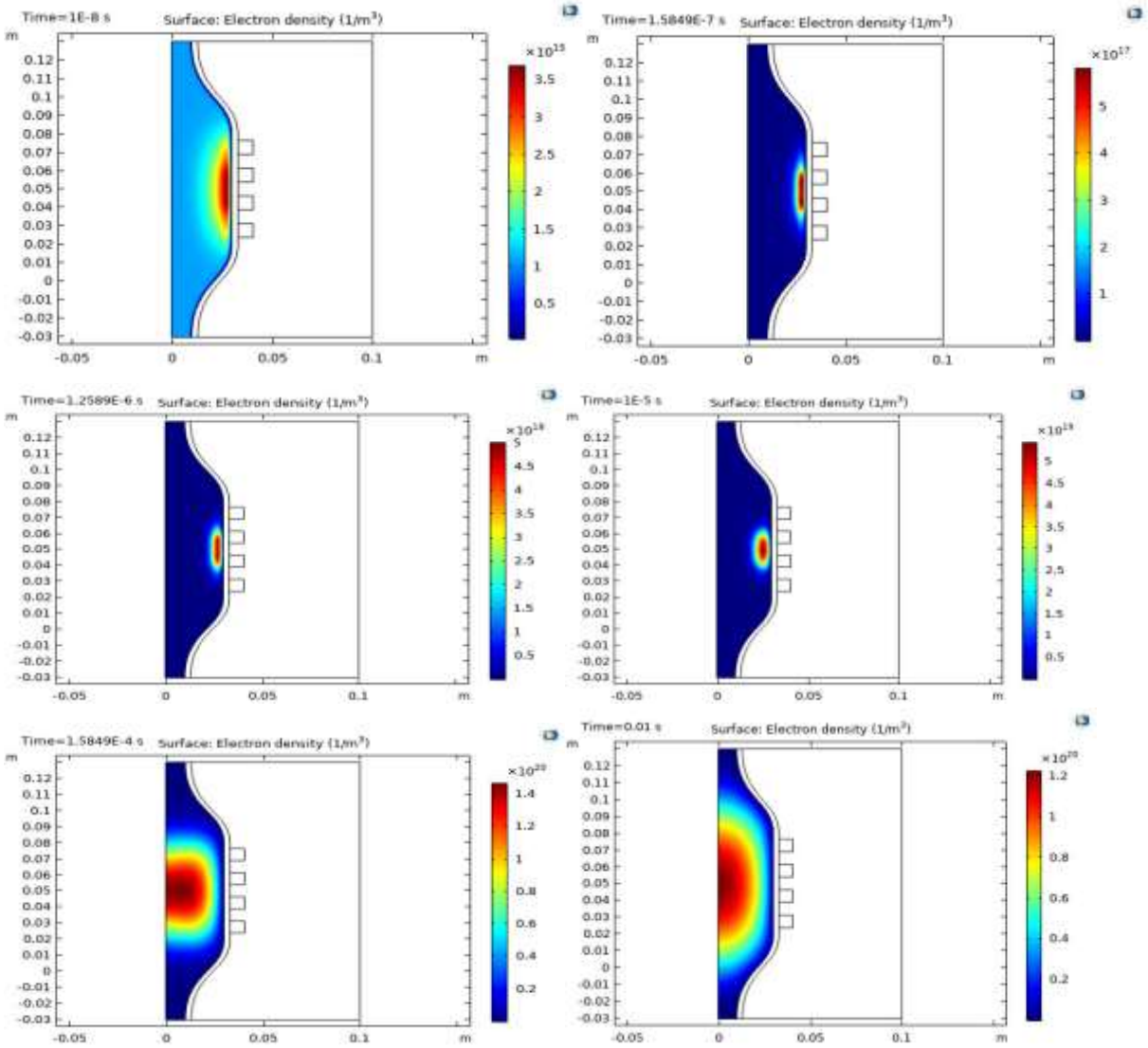

Figure 3. Electron density time evolution along the reactor coils inner part.

Figure 4 shows the electron temperature distribution behavior with time alone the reactor system. The electron temperature was 6 eV at the begins of simulation time and decreased with increasing time until reached 1.3 eV at 0.01 s. The distribution of electron temperature achieves the highest point in the core region, while dropping near the ICP wall. It can be found that electron number density and temperature shows a symmetrical distribution near the core of the reactor.

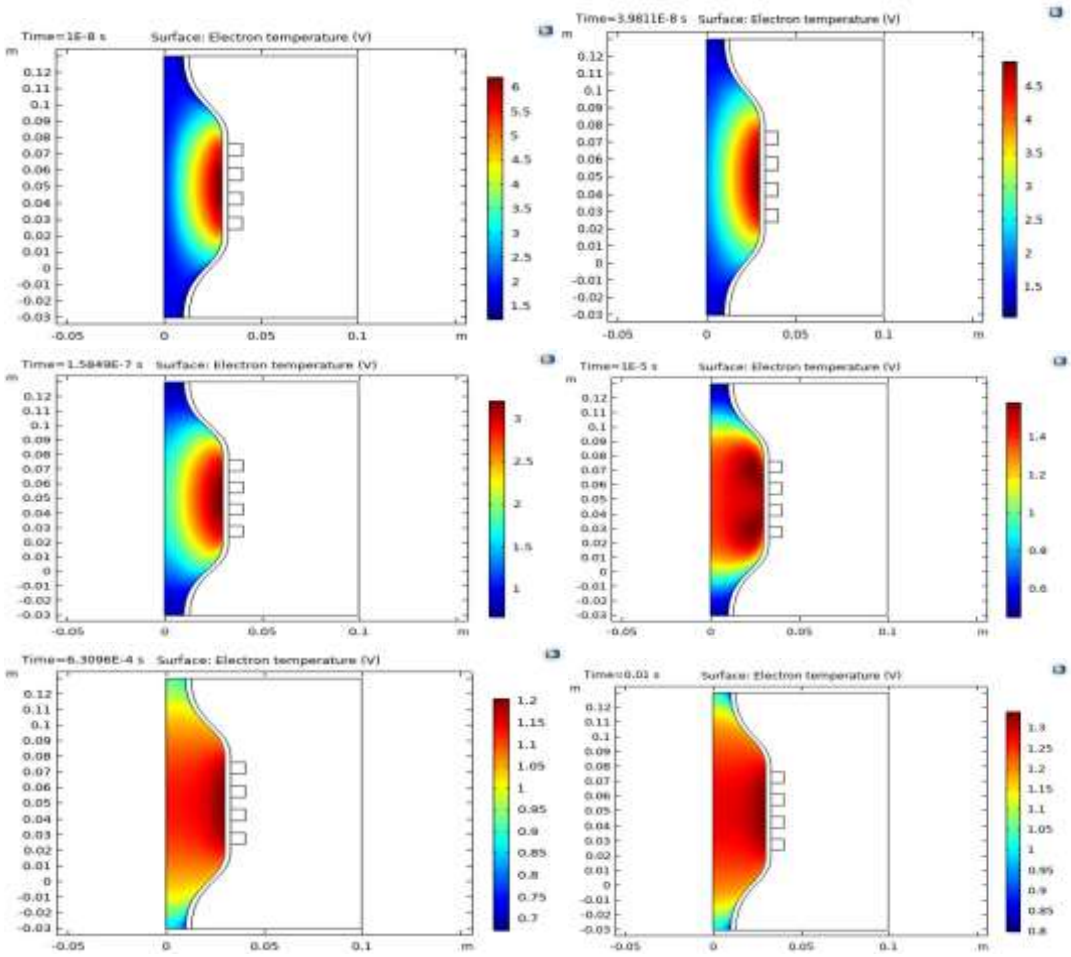

Figure 4. Electron temperature time evolution along the reactor coils inner part.

Figure 5 presents the surface distribution of electric potential in the chamber. The electric potential generated inside the chamber due to plasma action is found to be 18 V at time equal to 1×10^{-8} s and increased to 20 V after little time (1.7×10^{-8} s) then the potential decreased gradually and very slowly while it is spread in effect in the region of study and its maximum value is in the center of the chamber. At initial discharge, the potential increased and at peak applied voltage the potential reached maximum value. Late, afterglow, the potential decreased because only low energy ions hit the wafer as the plasma potential relaxes to less than 10 V.

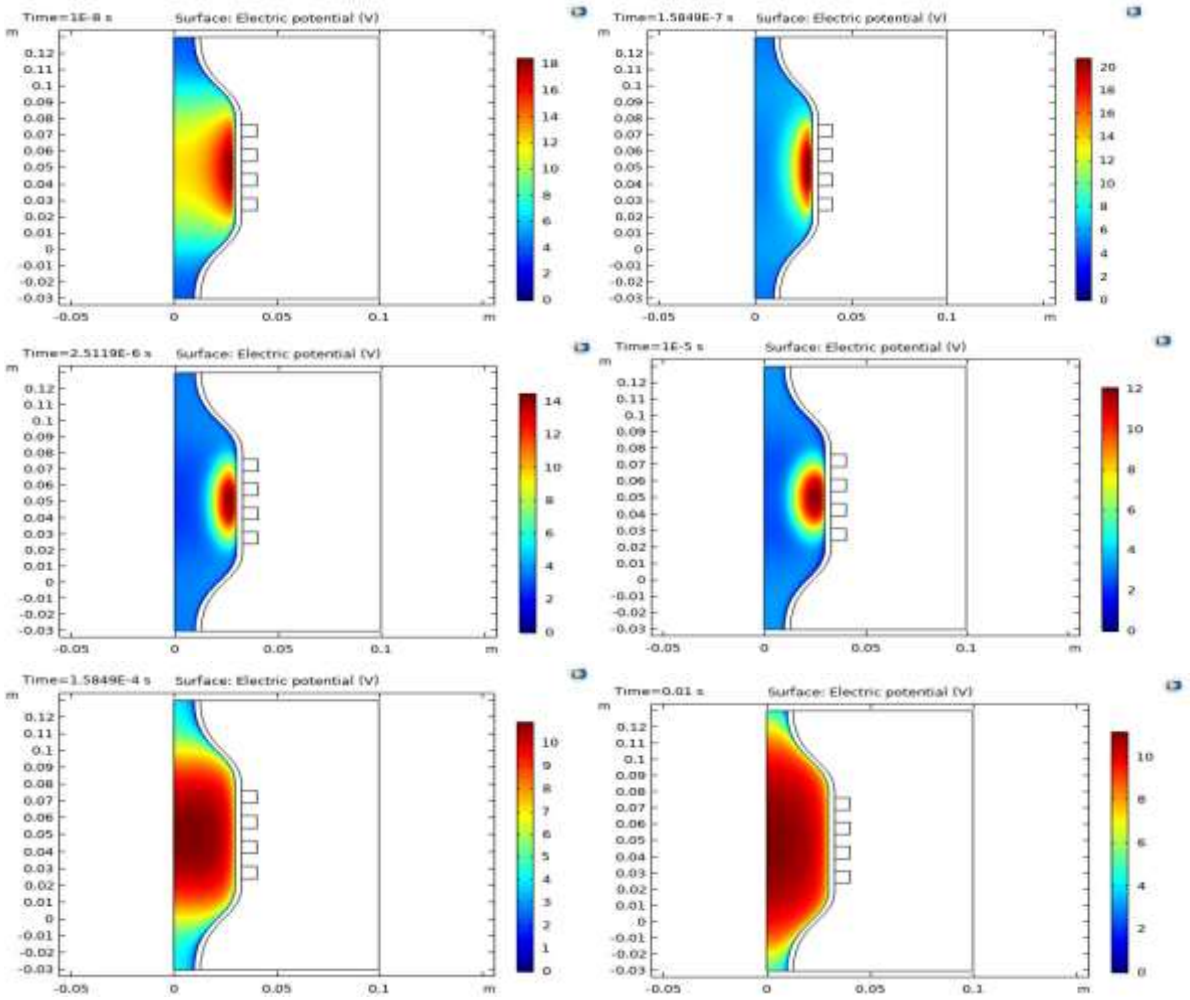

Figure 5. Time evolution of surface distribution of electric potential in the chamber.

The capacitive power deposition which is the focus of our work estimated. Figure 6 shows the capacitive power deposition (due to ions energy) in two lines, a, along the ICP chamber, and b, with time. From fig 5a, it is found that a symmetric power deposition density profile along the ICP chamber center. It reached maximum value equal to 1.25 $\times 10^8$ W/m^3. By calculating the system volume, the power equal to 5400 W. From fig5b, a time evolution of the power deposition density due to ions presents. As time of solution increased the deposited power density increased until reached maximum value then decreased slowly and seems to be semi constant. The power deposition importance comes from its relation to current of the reactor. The increasing in the reactor power means an increasing in the reactor current.

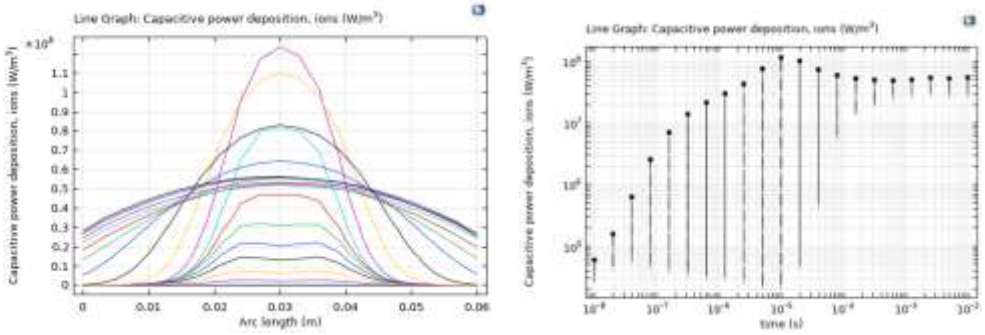

a. **b.**

Figure 6. The capacitive power deposition in the ICP reactor: a, along the ICP chamber, and b, with time.

During plasma formation mainly a type of losses take place namely Collisional Power Loss. Figure 7 shows the collisional power density loss with time of solution. From figure, as time increased the loss decreased sharply and very fast until reached or approach to zero, then it increased very little and be constants. Initially, the power dissipated in the coil. After about certain time, the plasma ignition begins and as the neutral gas atoms begin to free electrons and make ions, the electrons begin to absorb more and more power. At this time a counter current start flowing in the coil. The minus sign in the figure refer to as it is a loss. Results obtained in this paper is in good agreements with other studies [8,22].

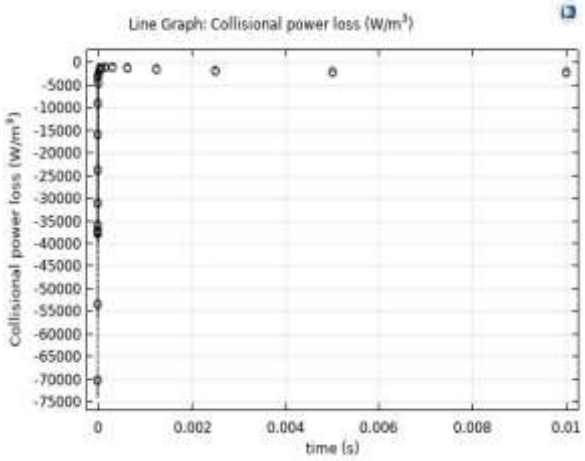

Figure 7. The collisional power loss in the ICP reactor with time.

3. Conclusions:

The numerical simulations of plasma reactors are useful for predicting plasma process and important in the performance of the reactor to be more active in plasma electrical applications. In the present paper, a two dimensional simulation performs a study of power deposition density in the inductively coupled plasma reactor using Comsol multiphysics solver. The study included some plasma parameters diagnostics which are electron temperature, electron number density, electric potential, power deposition and collisional power loss are obtained. Using mixture of two discharge gases which are the more dominate gas Ar that are used mostly in plasma, and the oxygen gas which have many active species. Results show that, as time increased the electron density increased which produce more energy and so increasing the power deposited.

4. References:

1. Marwa S. Hanon , Sabah N. Mazhir , Hazim I. al-Ahmed , Reem A. (2022), Influence of Non-Thermal Plasma (DBD) On Infertility Male Semen with Low Sperm Motility and Dna Damage, Iraqi Journal of Science, 2022, 63 (4).

2. Aiyah S. Noori , Kadhim A. Aadim , Alyaa H. Hussein (2022), Investigate and Prepare silver Nano Particles Using Jet PlasmaIraqi Journal of Science, 63 (6), p. 2461-2469.

3. Denise Adamoli Laroque , Sandra TiemiSeó , Germán AyalaValencia, João BorgesLaurindo, Bruno Augusto, MattarCarciofi (2022), Cold plasma in food processing: Design, mechanisms, and application, Journal of Food Engineering, 312.

4. Alyaa H. Ali, Zainab H Shakir, Alaa N. Mazher, Sabah N. Mazhir (2022), Influence of Cold Plasma on Sesame Paste and the Nano Sesame Paste Based on Co-occurrence Matrix, Baghdad science journal, 19 (4).

5. Thamir H Khalaf, Dawser H Ghayb (2021), Computational Study of Charge Density Produced in N2: H2 Plasma Actuator, Trends in Sciences 19 (9), p. 3476.

6. Dawser H Ghayb, Thamir H. Khalaf (2017), Inter. J. of Sci. and Research, 6 (11), p. 1561-1567.

7. Katarzyna Racka-Szmidt, Bartłomiej Stonio, Jarosław Zelazko, Maciej Filipiak, Mariusz Sochacki (2022), A Review: Inductively Coupled Plasma Reactive Ion Etching of Silicon Carbide, Materials, 15(123), p.1-23.

8. S Mouchtouris and G Kokkoris (2016), A hybrid model for low pressure inductively coupled plasmas combining a fluid model for electrons with a plasma-potential-dependent energy distribution and a fluid-Monte Carlo model for ions, Plasma Sources Sci. Technol. 25 (2), 025007.

9. T. Kimura, A. J. Lichtenberg, M. A. Lieberman (2001), Modelling finite cylinder electronegative discharges, Plasma Sources Sci. Technol. 10(3), 430.

10. Kortshagen, U., Gibson, N.D., Lawler (1996), On the E - H mode transition in RF inductive discharges, J.E., J. of Phys. D: Applied Phys., 29 (5), p. 1224.

11. Seo S.-H., Chung C., Chang, H.-Y. (2000), Review of heating mechanism in inductively coupled plasma, Surface and Coatings Technology, 131 (3), p. 1-11.

12. Zhao S.-X., Gao F., Wang Y.-N., J. of Phys. D: Appl. Phys., 42, 22(2009).

13. M. A. Lieberman and A. J. Lichtenberg (1994), Principles of Plasma Discharges and Materials Processing, , 1st edition, Wiley, New York.

14. D. P. Lymberopoulos and D. J. Economou (1995), Two-dimensional simulation of polysilicon etching with chlorine in a high density plasma reactor, IEEE Trans. Plasma Sci. 23 (4), p.573-580.

15. J. D. Bukowski , D. B. Graves (1996), Two-dimensional fluid model of an inductively coupled plasma with comparison to experimental spatial profiles, J. Appl. Phys., 80(2614).

16. P. L. G. Ventzek, T. J. Sommerer, R. J. Hoekstra, and M. J. Kushner (1994), Two-dimensional modeling of high plasma density inductively coupled sources for materials processing, J. Vac. Sci. Technol. B, 12(1), p. 461.

17. Denis Eremin (2016), Encyclopedia of Plasma Technology (1 st edition), Taylor & Francis, Boca Raton.

18. Horia Eugen Porteanu, Ilija Stefanovic, Nikita Bibinov, Michael Klute, Peter Awakowicz, Ralf Peter Brinkmann and Wolfgang Heinrich (2019), Correlated mode analysis of a microwave driven ICP source, Plasma Sources Science and Technology, 28 (3).

19. Hyo Chang Lee (2018), Review of inductively coupled plasmas: Nano-applications and bistable hysteresis physics, Applied Physics Reviews, 5 (011108).

20. Annemie Bogaerts, Erik C. Neytes (2018), Plasma Technology: An Emerging Technology for Energy Storage, ACS Energy Lett., 3 (4), p. 1013–1027.

21. Javadpour S. (2017), Simulation of magnetically confined inductively coupled plasma, M.Sc. Thesis, South Dakota State University, South Dakota.

22. Bozkurt E., Güngör Ü.E., and Alemdaroğlu N. (2017), Validation and benchmarking of COMSOL 2D axisymmetric inductively coupled argon plasma model, 9th Ankara International Aerospace Conference, p. 1-12.